

Characterization of field stitching in electron-beam lithography using moiré metrology

T. E. Murphy,^{a)} Mark K. Mondol, and Henry I. Smith

Massachusetts Institute of Technology, 60 Vassar Street, Cambridge, Massachusetts 02139

(Received 1 June 2000; accepted 25 July 2000)

We describe a method for characterizing field stitching in e-beam lithography systems. The method, which is based upon the moiré principle, enables one to measure interfield stitching errors to the nanometer level using only a conventional optical microscope. The technique is more sensitive than the commonly used vernier method, and it does not require the use of a coordinate-measuring tool. Our experiments show that this technique can determine the interfield stitching to within 2 nm.
© 2000 American Vacuum Society. [S0734-211X(00)00406-6]

I. INTRODUCTION

In all modern scanning-electron-beam lithography systems, large-area patterns are formed by stitching together a mosaic of small fields or stripes. Interfield stitching errors, the small unintended discontinuities which occur at the boundaries between adjacent fields, are major contributors to pattern-placement errors in e-beam lithography systems. This article describes a method for measuring and characterizing field stitching.

One of the most common ways of measuring pattern placement and field stitching is with a coordinate-measuring tool. In this approach, the e-beam system writes a sequence of marks, spanning many e-beam fields.¹ The sample is developed and the pattern transferred to the substrate. The coordinate-measuring tool locates the marks via optical microscopy as interferometry precisely measures the position of the stage. By comparing the measured position of each mark with its intended position, one can determine the pattern placement errors and field stitching. Unfortunately, coordinate-measuring tools are unavailable to many researchers; consequently, simpler means of evaluating stitching errors are needed.

Another commonly used technique for measuring stitching errors is to write a series of vernier marks along the edges of adjoining fields.² By inspecting the written vernier pattern in a scanning electron microscope, one can determine the amount of field stitching error between adjacent fields.

The method described here uses moiré metrology techniques to amplify interfield stitching errors to a level that can be easily measured with optical microscopy. This technique is far less expensive than using a coordinate-measuring tool, and more sensitive and more convenient than the commonly used vernier method.

The application of moiré techniques to nanolithography and nanometrology is not completely new. Moiré techniques have been used in the past to achieve nm-level mask alignment.³ Others have used moiré techniques to diagnose stitching errors and grating chirp in diffractive phase masks used in manufacturing fiber Bragg gratings.^{4,5} Recently, two-

dimensional moiré techniques have been used to provide *in situ* field calibration in an e-beam lithography system.⁶

II. MEASURING FIELD STITCHING WITH MOIRÉ METROLOGY

Our technique, illustrated in Fig. 1, uses a moiré pattern to measure the interfield stitching between two adjacent fields. Along the right edge of field 1, a fine-period grating of pitch p_1 is written. Along the left edge of field 2, a similar grating with pitch p_2 is written. The two fields are exposed with an intentional overlap, such that the two gratings are written on top of one another, as depicted in Fig. 1(b). When the sample is developed, a moiré pattern can be seen in the region of overlap. The pitch of the resulting moiré pattern is given by

$$P = \frac{p_1 p_2}{|p_1 - p_2|}, \quad (1)$$

where p_1 and p_2 are the pitches of the constituent gratings. It is important to point out that even if p_1 and p_2 are too small to be resolved optically, the moiré pattern can have a much larger periodicity which can easily be resolved in a conventional optical microscope.

The position (i.e., the spatial phase) of the moiré fringes depends very sensitively upon the relative placement of the two overlapping fields. A small stitching error between the fields will produce a magnified shift in the moiré pattern. By measuring the displacement of the moiré fringe pattern relative to its predicted position, one can precisely determine the interfield stitching error.

In order to measure the displacement of the moiré pattern, one must have a reference pattern which indicates where the moiré fringes would lie in the absence of any stitching error. To provide this, we include a set of reference moiré patterns immediately to the side of the overlapping region. These reference fringes are likewise created by superposing two periods (p_1 and p_2), however the constituent gratings are written entirely within a single e-beam field, ensuring that there is no appreciable placement error between them. Figure 2 illustrates the field pattern used for our moiré stitching measurements. The relative displacement of the middle moiré fringes with respect to the surrounding reference

^{a)}Electronic mail: tem@nano.mit.edu

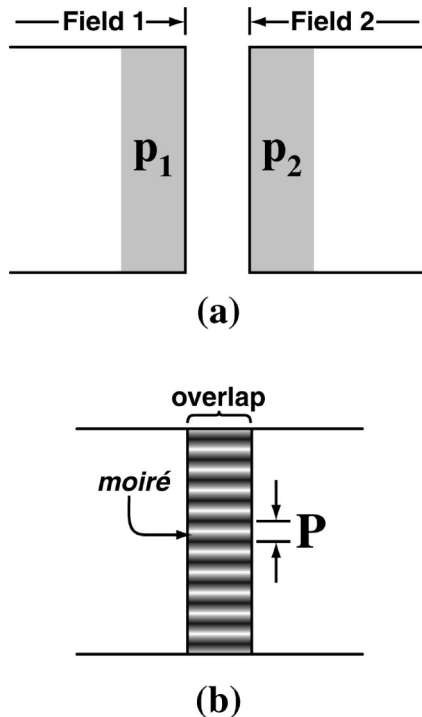


FIG. 1. Schematic of moiré technique used in stitching measurements. (a) depicts a fine-period grating with pitch p_1 along the right-hand edge of field 1, and a similar grating with pitch p_2 along the left-hand edge of field 2. When these two fields are written so as to overlap, as depicted in (b), a moiré pattern develops in the overlapping region.

fringes is indicative of a stitching error between the two fields. The displacement of the moiré fringes δ is related to the transverse stitching error Δy by

$$\delta = \Delta y \frac{P}{p_i}, \quad (2)$$

where p_i is either p_1 or p_2 , depending on whether the fringe offset is measured relative to field 1 or field 2. The magnification factor, P/p_i , expresses mathematically what was stated above: small interfield stitching errors cause a magnified shift in the moiré pattern.

One potential problem which can be easily seen in Fig. 2 is that there can be some ambiguity in the measurement of the fringe position: the fringe displacement can only be determined up to an integral number of fringe periods. In practice, however, one can usually place an upper limit on the stitching error. The grating periods p_1 and p_2 must then be chosen so that they are at least twice as large as the maximum anticipated stitching error. With this choice, the fringe displacement is guaranteed to fall between $-1/2$ fringe and $+1/2$ fringe. An alternative solution to this problem is to include a set of coarse marks alongside the moiré marks which would enable one to resolve the fringe ambiguity.

This method can provide a very sensitive measurement of the interfield stitching error. Additionally, there are some practical advantages to using this method. In comparison with conventional techniques, this method does not require any postexposure liftoff, etching, electroplating, or other pat-

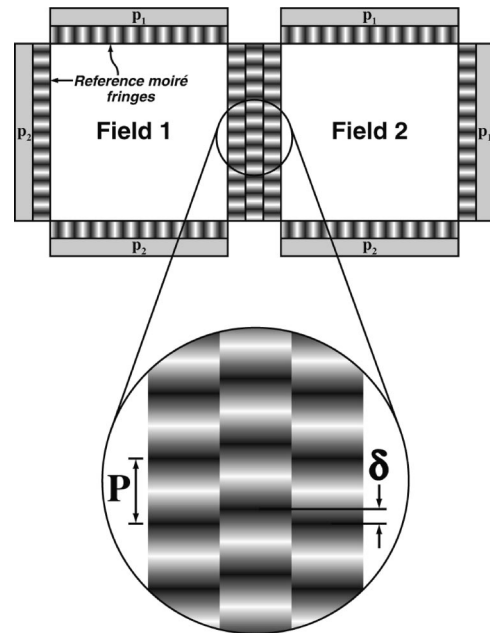


FIG. 2. Diagram of two partially overlapping e-beam fields. The reference moiré patterns located on either side of the overlapping region provide a basis for measuring the relative position of the moiré fringes, i.e., the spatial-phase shift of the overlapping region.

tern transfer: the moiré images can be seen directly in the developed (or even partially developed) resist. Also, the written test patterns do not need to be examined in a high-resolution microscopy tool, such as a scanning-electron microscope or atomic-force microscope. Because of these advantages, one could imagine routinely writing a small array of test fields alongside real device patterns, providing a useful diagnostic for the stitching performance. Since the measurement relies on nothing more than resist development and optical microscopy, the stitching measurement is guaranteed to be compatible with subsequent sample processing.

III. EXPERIMENTAL PROCEDURES

In order to demonstrate the capabilities of this technique, we have performed several stitching experiments using our VS2A e-beam lithography system. For all the tests, we used wafers with 250 nm thick poly(methylmethacrylate) (PMMA).

Table I lists the important parameters used for the measurements on 100 and 400 μm fields. The fine-period gratings (p_1 and p_2) were written as arrays of one dimensional lines. From prior independent measurements of the stitching

TABLE I. Parameters used for the moiré stitching measurements on 100 and 400 μm fields.

Field size	Address increment	p_1	p_2	P
100 μm (16 384 pixels)	6.10 nm (1 pixel)	189.2 nm (31 pixels)	195.3 nm (32 pixels)	6.055 μm (992 pixels)
400 μm (16 384 pixels)	24.4 nm (1 pixel)	293.0 nm (12 pixels)	317.4 nm (13 pixels)	3.808 μm (156 pixels)

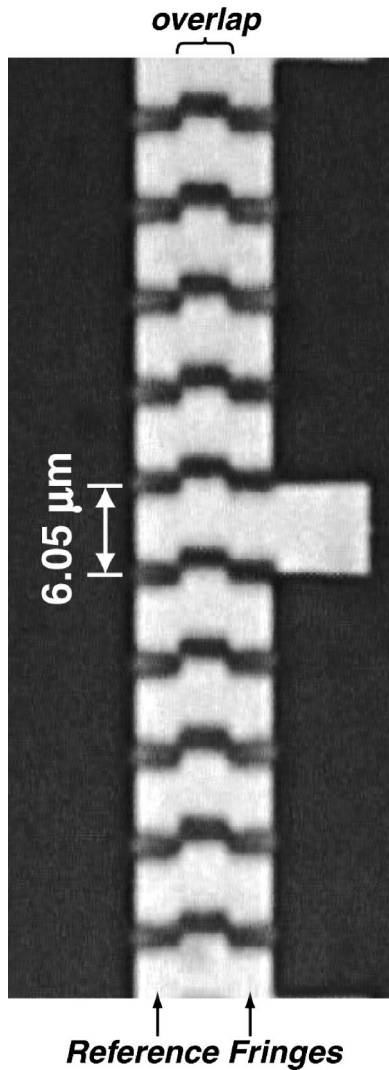


FIG. 3. Optical micrograph showing moiré fringes at the boundary between two $100\ \mu\text{m}$ fields. This image was captured using a CCD camera connected to a conventional optical microscope, through a $20\times$, 0.4 numerical aperture differential-interference-contrast objective lens. The period of the moiré pattern is approximately $6.05\ \mu\text{m}$. The clear displacement of the middle moiré fringes with respect to the surrounding reference fringes is indicative of a transverse stitching error between these fields.

performance of our system, we knew that the stitching error seldom exceeds $80\ \text{nm}$ for $100\ \mu\text{m}$ fields and $150\ \text{nm}$ for $400\ \mu\text{m}$ fields. The grating periods p_1 and p_2 listed in Table I were chosen with these limits in mind, ensuring that the moiré fringe discontinuity will be less than $1/2$ fringe.

For some fields, we included a set of vernier marks alongside the moiré fringes, allowing us to compare the moiré technique with the more commonly used vernier method. A variety of doses were used to identify the optimal dose for generating moiré patterns.

The samples were developed in a solution of 60:40 IPA: MIBK for $60\ \text{s}$, and inspected in an optical microscope. Figure 3 is a representative optical micrograph showing the moiré fringes at the boundary between two adjacent $100\ \mu\text{m}$ fields. Three moiré bands are clearly visible in Fig. 3: the outer two bands are the reference fringes, and the middle

band is where the adjacent fields overlap. The stitching error between these two fields is evidenced by the visible displacement of the middle moiré fringe pattern with respect to the surrounding reference fringes.

The optimal line dose was found to be $1.9\ \text{nC/cm}$ for both the 100 and $400\ \mu\text{m}$ fields. Note that these dose figures refer to the constituent grating lines considered separately—in those places where grating lines overlap (i.e., at the peaks of the moiré fringes) the delivered dose is actually twice as high. We found that moiré patterns can still be seen and measured in the developed resist even if the dose is changed by $\pm 10\%$. Additionally, the moiré patterns can be seen even in partially developed resist.

IV. STITCHING MEASUREMENT AND DATA ANALYSIS

From the optical micrograph in Fig. 3, one can estimate the relative fringe offset to approximately $P/10$, by visual inspection alone, which corresponds to a measurement uncertainty of about $20\ \text{nm}$ for the $100\ \mu\text{m}$ fields. However, one can obtain a more precise estimate of the fringe offset by numerically analyzing the fringe patterns, as will be described.

First, the optical micrographs are recorded on a charge coupled device (CCD) camera and converted to 16-bit grayscale images, where the light intensity at each pixel is stored as a non-negative integer ranging from 0 to 65535. The position of the moiré fringes can then be estimated using a spectral analysis technique. Each vertical column of pixels in the optical moiré image may be regarded as a length N discrete periodic signal, which we denote $\phi[n]$. The discrete Fourier transform (DFT) of this signal is given by

$$\Phi(\omega) = \sum_{n=0}^{N-1} \phi[n] e^{-j\omega n}. \quad (3)$$

The spectrum $\Phi(\omega)$ of the data has a peak at a frequency ω_0 which corresponds to the spatial frequency of the moiré pattern:

$$\omega_0 = \arg \max_{\omega} |\Phi(\omega)|^2. \quad (4)$$

The phase of the spectrum at its peak value represents the position of the moiré fringe, i.e.,

$$\theta = \tan^{-1} \left(\frac{\text{Im}[\Phi(\omega_0)]}{\text{Re}[\Phi(\omega_0)]} \right). \quad (5)$$

The spectrum in Eq. (3) can be very efficiently computed using the fast Fourier transform (FFT) algorithm, after zero-padding the data sequence to a sufficient length. This analysis can be carried out for each column of data comprising the image, which allows one to plot a profile of the moiré phase across the boundary. Figure 4 plots such a phase profile for the field boundary shown in Fig. 3.

Based upon the signal-to-noise ratio in the optical micrograph, we believe that the spectral technique described can determine the phase of the moiré fringe to better

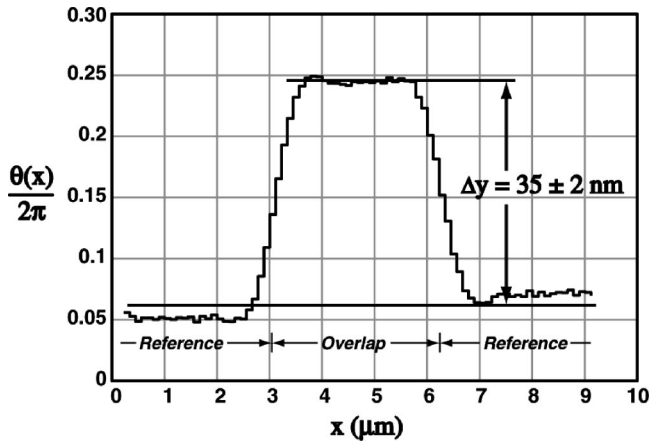


FIG. 4. Computed spatial-phase profile for the moiré image shown in Fig. 3. The phase (position) of the moiré fringes is calculated using a FFT-based method. The middle moiré fringes are displaced with respect to the surrounding reference patterns by 0.18 fringes. From this, we determine that the interfield stitching error is 35 ± 2 nm.

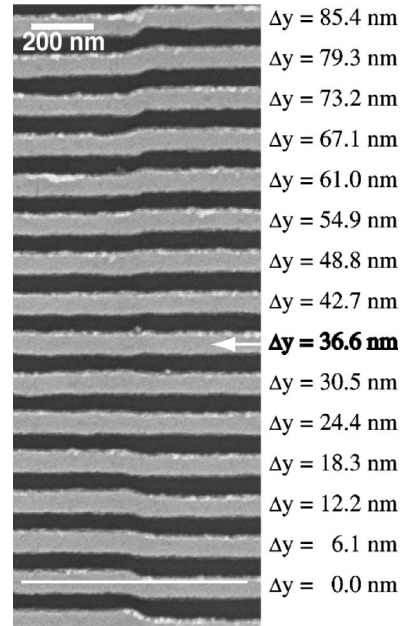
than $P/200$. However, the precision of the measurement technique is limited by other factors described as follows.

The phase profile plotted in Fig. 4 shows a clear discontinuity of approximately 0.18 fringes between the middle moiré pattern and the adjacent reference fringes, which corresponds to a stitching error of 35 nm. Notice that there is a small discrepancy between the measured phase of the two reference fringes. This phase discrepancy arises for two reasons. First, as there is a stitching error of about 35 nm between the two fields, the reference moiré fringes from each field should not be expected to line up exactly. The relationship between the two fringe discontinuities and the transverse stitching error is

$$\delta_1 = \Delta y \frac{P}{p_1}, \quad \delta_2 = \Delta y \frac{P}{p_2}, \quad (6)$$

where δ_1 represents the left-hand side fringe discontinuity and δ_2 represents the right-hand side fringe discontinuity. For the 100 μm field parameters listed in Table I, Eq. (6) predicts that δ_1 should always be 3.2% larger than δ_2 . (In fact, it is possible to use this predictable discrepancy between the left-hand side and right-hand side reference fringes to remove the ambiguity from the measurement of the fringe offset.) However, this factor only accounts for part of the discrepancy seen in Fig. 4.

We attribute the remaining discrepancy to intrafield placement errors which are introduced while the reference moiré patterns are being written. If, when patterning the reference moiré pattern, there is any drift in pattern placement between when the two component gratings p_1 and p_2 are written, the reference moiré fringe will be displaced from its nominal position. Such intrafield pattern placement errors can arise, for example, from charging of the sample, differential thermal expansion, or a variety of other sources of drift. Based upon our observations of the moiré fringes, we believe that



vernier measurement:
 $\Delta y = 37 \pm 6$ nm

FIG. 5. SEM showing vernier marks written at the boundary between two e-beam fields. These marks were written along the same field boundary depicted in Fig. 3. The interfield stitching error, as measured from these vernier marks, is found to be 37 ± 6 nm. This agrees with the moiré method, but has a larger measurement uncertainty.

these intrafield deviations can be as large as 2 nm. This effect is what limits the accuracy of the moiré measurement scheme in our system to about ± 2 nm.

As mentioned earlier, in order to verify the stitching measurement, we wrote a set of vernier marks alongside the moiré patterns. Figure 5 is a scanning electron micrograph (SEM) showing labeled vernier marks which were written along the same boundary shown in Fig. 3. Prior to inspecting the vernier marks in the SEM, we lifted off 40 nm of chromium to provide image contrast, and we also sputter coated the sample with gold to prevent charging. For simplicity, the vernier marks were written with the same period (p_1 and p_2) as the moiré gratings. The difference in vernier pitch is exactly one pixel, which provides the maximum vernier sensitivity attainable for our e-beam tool.

As shown in Fig. 5, the vernier marks reveal a stitching error of 37 ± 6 nm. In contrast, the moiré method measures the stitching error to be 35 ± 2 nm. The two methods are in agreement, but the moiré method provides a more precise measure than the vernier method and does not require pattern transfer and SEM analysis.

Although we have not sought in this work to minimize the size of the moiré marks, it is worth comparing the amount of space consumed by the moiré method and vernier method. The pitch of the vernier marks in Fig. 5 is approximately 200 nm, with a difference in pitch of only one pixel (i.e., 6.10 nm) between the left-hand side and right-hand side gratings. Given these parameters, in order for the vernier marks to have the same measurement range as the moiré technique,

the total length of the vernier marks must be approximately $6\ \mu\text{m}$ (i.e., approximately one moiré fringe.) In comparison, we have found that the moiré technique requires about three fringes in order to reliably determine the stitching error. The width of the vernier marks is likewise somewhat smaller than that of the moiré marks. From the phase profile depicted in Fig. 4, we infer that the full width of the moiré regions could probably be reduced to about $4\text{--}5\ \mu\text{m}$ without significantly affecting the measurement accuracy. Further reduction in size could be achieved were one to use a microscope objective with higher resolution (better than $NA=0.4$). Thus, although the vernier marks consume somewhat less real estate, the space required by the moiré technique is still quite modest, and the measurement precision achieved with the moiré technique is superior.

V. CONCLUSIONS

We described a technique, based upon the moiré principle, for measuring interfield stitching errors in e-beam lithography systems. This technique allows one to measure the interfield stitching error using only a conventional optical

microscope. With relatively simple off-line image-processing techniques, this technique can unambiguously determine the interfield stitching error to about $\pm 2\ \text{nm}$. We believe this technique is more convenient and more sensitive than other commonly used techniques.

ACKNOWLEDGMENTS

The authors acknowledge the many helpful suggestions and comments from J. T. Hastings and J. Goodberlet regarding e-beam placement accuracy and moiré metrology. This work was sponsored by AFOSR, DARPA, and ARO.

¹K.-D. Roth and K. Rinn, *Leitz Sci. Tech. Inform.* **11**, 130 (1997).

²B. H. Koek, T. Chrisholm, J. Romijn, and A. J. van Run, *Jpn. J. Appl. Phys., Part 1* **33**, 6971 (1994).

³A. Moel, E. E. Moon, R. Frankel, and H. I. Smith, *J. Vac. Sci. Technol. B* **11**, 2191 (1993).

⁴F. Barnier, P. E. Dyer, H. V. Snelling, and R. M. De la Rue, *Opt. Commun.* **170**, 175 (1999).

⁵F. Barnier, P. E. Dyer, and G. A. Steigmann, *Opt. Commun.* **162**, 299 (1999).

⁶J. T. Hastings, F. Zhang, M. Finlayson, J. G. Goodberlet and H. I. Smith, *J. Vac. Sci. Technol. B*, these proceedings.